Proceedings of the 26th Annual International Conference of the IEEE EMBS
San Francisco, CA, USA • September 1-5, 2004

Validation of Adaptive Threshold Spike Detector for Neural Recording

Paul T. Watkins[1], Gopal Santhanam[2], Krishna V. Shenoy[2,3], and Reid R. Harrison[1]
[1]Department of Electrical and Computer Engineering, University of Utah, Salt Lake City, Utah, USA
[2]Department of Electrical Engineering, [3]Neurosciences Program, Stanford University, Stanford, California, USA

Abstract—**We compare the performance of algorithms for automatic spike detection in neural recording applications. Each algorithm sets a threshold based on an estimate of the background noise level. The adaptive spike detection algorithm is suitable for implementation in analog VLSI; results from a proof-of-concept chip using neural data are presented. We also present simulation results of algorithm performance on neural data and compare it to other methods of threshold level adjustment based on the root-mean-square (rms) voltage measured over a finite window. We show that the adaptive spike detection algorithm measures the background noise level accurately despite the presence of large-amplitude action potentials and multi-unit hash. Simulation results enable us to optimize the algorithm parameters, leading to an improved spike detector circuit that is currently being developed.**

Keywords—**Spike detection, integrated circuit, neural recording, action potential**

I. Introduction

Current research in neuroscience and neuroengineering often involves the simultaneous recording of many neurons. To this end, arrays of 100 microelectrodes have been developed for extracellular neural recording, and it is anticipated that even larger arrays will be used in the near future [1]. Such electrode arrays will soon be part of fully implantable neural recording systems. In scientific and clinical (i.e., neuroprosthetic) applications, it is necessary to identify neural action potentials ("spikes") from the voltage waveform of each electrode. Spike detection may be used for data reduction by merely reporting the presence of a spike rather than digitizing the electrode voltage waveform. Alternatively, spike detection may be used as part of a system to trigger limited recording over some time window around each spike.

A simple thresholding mechanism is often used to detect spikes. Both the large number of electrodes and the implanted nature of future systems make automatic threshold level adjustment desirable compared to manually setting the threshold for each channel.

This work was supported by a National Science Foundation CAREER award (ECS-0134336, R.R.H.), the University of Utah Wayne Brown Fellowship (P.W.), an NDSEG fellowship (G.S.) and the following awards to K.V.S.: NSF Center for Neuromorphic Systems Engineering at Caltech, ONR Adaptive Neural Systems, Whitaker Foundation, Center for Integrated Systems at Stanford, Sloan Foundation, and Burroughs Wellcome Fund Career Award in the Biomedical Sciences. Please address correspondence to harrison@eng.utah.edu.

Traditionally, spike-detection thresholds are set by measuring the rms voltage of a signal over some brief time window (e.g., 250 ms) and using a multiple of this voltage as the threshold [1]. This "direct rms measurement" method is susceptible to bias due to the presence of large-amplitude spikes, which inflate the estimate of rms noise level. Also, background noise may not be stationary [2], requiring repeated measurements or some other automatic threshold scheme capable of tracking the noise level and setting the threshold accordingly.

We recently presented a spike detector circuit which adaptively sets its detection threshold according to the background noise level [3]. This fully-integrated, low-power VLSI circuit implemented a novel algorithm to estimate the rms voltage level of Gaussian noise ($V_{1\sigma}$) and set a threshold to an integer multiple of this voltage ($V_{N\sigma}$). A proof-of-concept chip was tested and initial results using synthetic data were presented.

If the measured signal is strictly a realization of a stationary Gaussian noise process, both the traditional "direct rms measurement" and the adaptive spike detection algorithm proposed in [1] will yield equivalent threshold levels. However, the presence of large-amplitude action potentials reduces the accuracy of both algorithms. Furthermore, there is evidence that a *t*-distribution is a better model for neural background noise than a Gaussian distribution [4]. Thus, both the direct rms measurement method and the adaptive spike detection algorithm will give *approximate* measures of background noise levels.

In this paper, we compare the performance of these algorithms using actual neural data recorded from a microelectrode array in monkey pre-motor cortex. We demonstrate operation of the chip described in [3] on the neural data, and we explore the operation of both algorithms in simulation.

II. Adaptive Spike Detection Algorithm

The adaptive spike detection algorithm attempts to set a threshold to detect neural spikes in the presence of background noise, while avoiding false positives due to occasional peaks in the noise. This algorithm was developed with the assumption that the input to the system consists of spikes added to band-limited white Gaussian noise. As shown in Fig. 1, if band-limited white Gaussian noise is fed into a comparator with a threshold set at one standard deviation of the noise, the probability of exceeding the threshold is 0.159. Thus, the reference level of the comparator should be adjusted so that the comparator's output has a duty cycle of 15.9%.

Fig. 2 shows the basic feedback control loop, which uses proportional control to adjust the threshold of Comparator A until its output has a duty cycle of 15.9%. This corresponds to a threshold set at one standard deviation ($V_{1\sigma}$). A gain stage sets the threshold of Comparator B to a multiple of this voltage: $V_{N\sigma}$. If N is set to 3 or higher, comparator B should then detect spikes while rejecting noise with a high probability since Gaussian noise rarely exceeds three times its rms value. A higher value of N can be chosen for a more conservative threshold.

In a proportional control system, the feedback signal is proportional to the current error; in such a system, a steady-state error is required to maintain a non-zero control signal. To eliminate the steady-state error and thus improve the accuracy of the algorithm, proportional integral control can be introduced; this is explored in simulations below.

Note that the presence of spikes will reduce the accuracy of the rms measurement, but in a weak manner. Specifically, the large-amplitude spikes do not affect the algorithm any more than small-amplitude spikes since they both exceed the 1σ threshold. The difference in duration of small- and large-amplitude spikes has a negligible impact on the threshold level.

III. Neural Dataset

To test spike detection algorithms under realistic conditions, we used an extracellular neural recording dataset. The data were acquired from one electrode of a 100-channel silicon microelectrode array using a Cerebus data acquisition system (Cyberkinetics, Inc.). The electrode array was implanted at the border of the M1 and PMd regions of a rhesus monkey's right cortical hemisphere. The data were bandpass filtered with corner frequencies 0.3 Hz and 7.5 kHz, then sampled at 30 kS/s, digitized to 12-bit accuracy, and saved for further processing. The data were subsequently high-pass filtered at 250 Hz (4^{th}-order) to remove local field potentials. The data were also inverted to accommodate the positive range of the spike detector.

The dataset consists of a 120-second record of the voltage on a single microelectrode. In this recording, several spiking units are visible. Using the Cerebus software the electrode was hand sorted with a time-amplitude hoop scheme and three distinct spike waveforms were identified. Average spike shapes for these units are presented in Fig. 3, where it can be seen that these have a wide range of average peaks: 573 μV, 240 μV, and 85 μV. The data were further processed offline using an unsupervised spike sorting algorithm [5], which clusters the data using a version of the Expectation-Maximization algorithm, after having aligned the spikes' peaks and performing principle component decomposition. This algorithm verified that units 1 and 2 were individual units, but found that the remaining unit was actually a multiunit consisting of three neurons with very similar spike shapes.

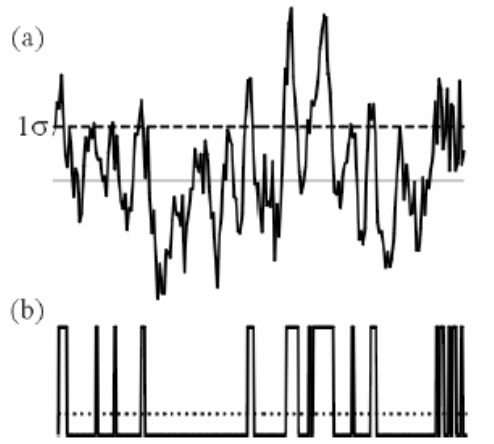

Fig. 1. (a) If Gaussian noise is passed through a comparator having a threshold set to the rms value of the noise (1σ), the resulting digital signal (b) made up of 0's and 1's has a dc level (dotted line) of 0.159.

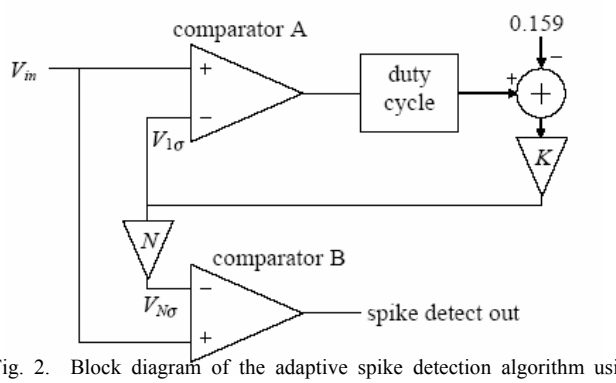

Fig. 2. Block diagram of the adaptive spike detection algorithm using proportional feedback control.

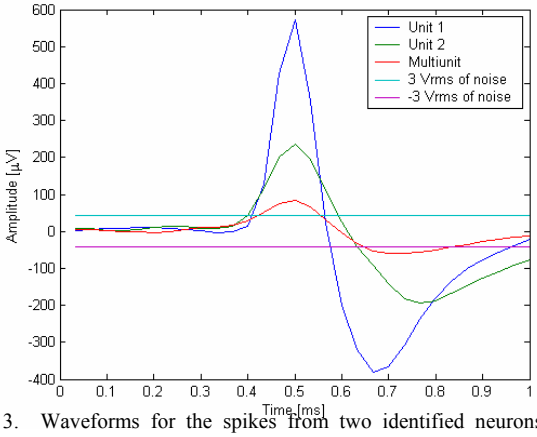

Fig. 3. Waveforms for the spikes from two identified neurons and a multiunit in our 2-minute data set. Each waveform is an average of 10 individual spikes. The background noise level is also indicated for reference.

To measure the level of the background noise in the recording, we removed a 2 ms window around all identified spikes from the data. From the remaining data, we measured a background noise rms value of 15.3 μV. Fig. 4 shows a histogram of this background activity compared with a Gaussian noise histogram with the same rms value. A histogram of the original data is also included for

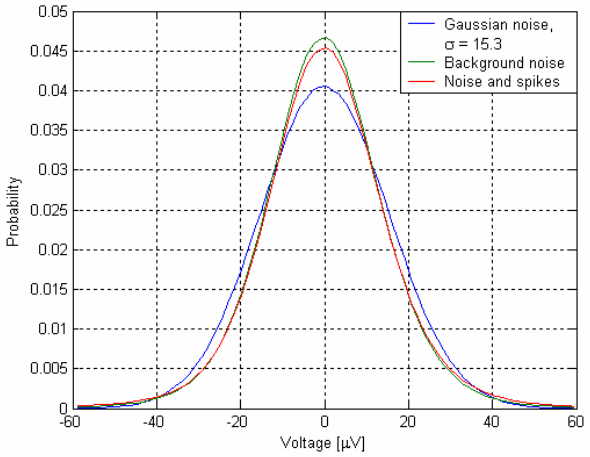

Fig. 4. Histograms of background noise in neural data, Gaussian noise with a standard deviation of 15.3 μV, and the full data set.

comparison. It can be seen that the background noise does not match Gaussian noise very well at the edges of the distribution (Gaussian noise with a standard deviation of 13.2 μV was a better fit). In both cases, the background noise has wider tails than the Gaussian distributions. However, we expect the adaptive spike detection algorithm to perform robustly despite this discrepancy.

IV. Results

To verify the circuit implementation of our adaptive spike detection algorithm [3] we played the neural dataset through a PC sound card connected to our chip. The chip implemented the system shown in Fig. 2 with $N = 5$. The neural data was amplified by 60 dB. (In a complete neural recording system, a preamplifier would precede the spike detector.) An example of the chip's performance is shown in Fig. 5, which shows the neural data, the threshold $V_{5\sigma}$, and the spike detector output. The $V_{5\sigma}$ signal exhibits glitches due to the clocked comparators, but these do not affect the chip's performance (i.e., the glitches do not cause spurious detections). The spike detector chip adapts to a threshold of $V_{5\sigma} = 53$ mV. This corresponds to an rms noise level of $V_{1\sigma} = 10.6$ mV, which is 30% lower than the actual background noise in the neural data. The chip's performance was limited by this inaccuracy as it sometimes triggered on the background noise (data not shown). This inaccuracy was caused by the small gain of the feedback control loop (K), which was approximately 2.5 V/V. This performance is consistent with our simulations, which showed that lower loop gains resulted in lower threshold levels.

In simulation, we compared the performance of four different methods for estimating the rms background noise level: the adaptive spike detection method with proportional (P) feedback control as shown in Fig. 2, the same algorithm with proportional-integral (PI) feedback control, a direct rms measurement over a 250 ms window as used in [1], and a direct rms measurement over a 1000 ms window.

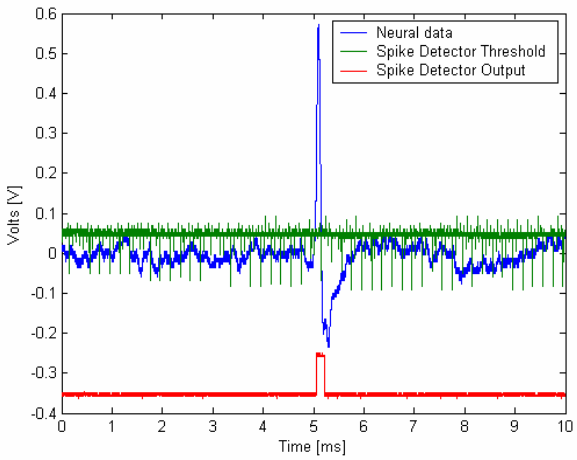

Fig. 5. Measured performance of spike detector chip on neural data. The neural data, the threshold $V_{5\sigma}$ set by the chip, and the spike detected signal are shown. The $V_{5\sigma}$ signal exhibits glitches due to the clocked comparators in the chip, but these do not affect chip performance.

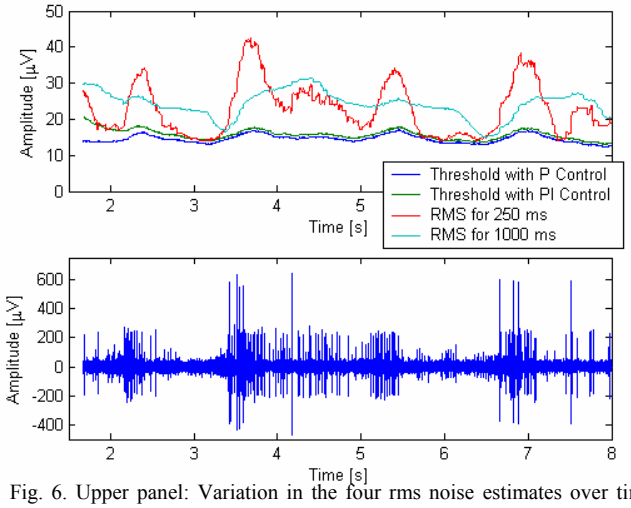

Fig. 6. Upper panel: Variation in the four rms noise estimates over time. These values would be scaled by a factor of N to be used as spike detection thresholds. Lower panel: high pass filtered, inverted neural data.

In our simulations, we used a first order Chebyshev low-pass filter with a cutoff frequency of 0.01 Hz to measure the duty cycle of comparator A (see Fig. 2). For the proportional gain, K, we used 10 V/V, which was four times higher than the gain implemented in the spike detector chip [3]. For PI control, we used the same proportional gain and an integral gain of 0.0025 V/V·s. Finally, we set $N = 5$. We used the Cerebus detection and classification software as a reference for comparing these methods.

We ran simulations on the 120-second neural dataset. The adaptive spike detection algorithm had an initial transient response that lasted 1.5 seconds; simulation results for this period are not shown. Fig. 6 shows how the rms noise level estimates ($V_{1\sigma}$ or V_{rms}) behaved over a period of 6.5 seconds. We see that the adaptive spike detection algorithm is much less affected by occasional bursts of spikes than the direct rms measurement methods. This is

TABLE I
Comparison of noise level measurement methods
(True rms level of neural background noise was 15.3 μV.)

	Mean (μV)	Max (μV)	Min (μV)	Std. Dev. (μV)
P	13.6	18.5	9.9	1.79
PI	14.3	20.8	9.8	1.94
RMS (250)	19.2	45.5	9.9	6.39
RMS (1000)	19.7	34.9	11.2	4.89

TABLE II
Spike detection performance for $N = 5$

	P	PI	RMS 250	RMS 1000	True RMS
Unit 1	100%	100%	100%	100%	100%
Unit 2	100%	100%	100%	100%	100%
Multiunit	91.3%	84.9%	45.3%	45.1%	87.2%
Other Crossings	648	480	204	211	237

because the adaptive algorithm only uses the *frequency* of threshold crossings to estimate noise level and is unaffected by the large amplitude of the spikes.

Next, we compared the performance of these four algorithms over the full 120-second neural dataset. The results of these simulations are shown in Table I. The mean, minimum, and maximum values of the rms noise level estimates given by each algorithm are presented, along with the standard deviation.

From the data in Table I, we see that the mean values produced by both the P and the PI adaptive spike detection methods provide good estimates for the true rms voltage of the background noise, which was measured to be 15.3 μV (see Section III). We also see that the addition of integral control (PI) has improved performance somewhat (the duty cycle of comparator A reached 15.9%), but the threshold is still lower than the measured background rms value. This inaccuracy is due to the presence of spikes and non-Gaussian noise. The direct rms measurement methods overestimate the noise and exhibit more variation because they are strongly affected by high-amplitude spikes in the signal.

Simulations were run to see how well thresholds set to five times the estimated rms noise level ($N = 5$) detected the spikes present in the neural dataset. For comparison, we also included a threshold set to five times the true background noise rms voltage of 15.3 μV. In Table II, we present the percentage of the classified units correctly detected, and also the number of threshold crossings not due to the classified units. In our 120-second dataset, unit 1 fired 80 times, unit 2 fired 970 times, and the multiunit fired 1637 times. As expected, the spike detection algorithm detected the large amplitude spikes. The multi-unit was detected approximately 90% of the time by the P and PI methods, however these methods were also subject to a large number of threshold crossings not due to classified units. Using $N = 5$ would thus work well in a system using a spike detector to trigger spike sampling. If the spike detector were being used in isolation, a higher value of N should be used, and only the two large amplitude units would be detected. Simulations using $N = 7$ detected the two large-amplitude units 100 percent of the time, with very few threshold crossings not due to classified units (on the order of 10 per minute). The rms methods set higher thresholds due to their overestimation of the noise. The higher thresholds detect the large amplitude spikes, but less than half of the multi-unit activity.

V. CONCLUSION

We have presented measurements from an adaptive spike detector chip using actual neural data. We further investigated the performance of the proposed adaptive spike detection algorithm in simulations. We have shown that the thresholds generated by our algorithm are less variable in the face of large-amplitude spikes than are other methods based on direct measurement of the rms waveform voltage.

The current adaptive spike detector chip first presented in [3] has a loop gain too low for the desired accuracy. Simulations show that a higher gain would improve performance considerably. The used of PI control instead of simple P control also improves performance, but the additional complexity of adding integral control may not be warranted, as the performance increase is small.

We are currently designing an improved spike detector chip with higher loop gain, which should improve performance considerably. The chip will also have a programmable value of N, in the range of 3 to 7, which will allow the user to set N lower if the spike detector is used for trigger sampling (e.g., a "snapshot" of each spike), or higher if the spike detector is being used only to identify large-amplitude spikes.

REFERENCES

[1] K. S. Guillory, R. A. Normann, "A 100-channel system for real time detection and storage of extracellular spike waveforms," *J. Neuroscience Methods*, vol. 91, pp. 21–29, 1999.

[2] M. S. Fee, P. P. Mitra, D. Kleinfeld, "Variability of Extracellular Spike Waveforms of Cortical Neurons," *J. Neurophysiology*, vol. 76(6), pp. 3823–3833, 1996.

[3] R. R. Harrison, "A Low-Power Integrated Circuit for Adaptive Detection of Action Potentials in Noisy Signals," in *Proc. 2003 Intl. Conference of the IEEE Engineering in Medicine and Biology Society*, Cancun, Mexico, Sept. 2003.

[4] S. Shoham, M. R. Fellows, R. A. Normann, "Robust, automatic spike sorting using mixtures of multivariate t-distributions," *J. Neuroscience Methods*, vol. 127, pp. 111-122, 2003.

[5] M. Sahani, "Latent Variable Models for Neural Data Analysis." Ph.D. Dissertation, Computation and Neural Systems. California Institute of Technology, 1999.